A Threshold-Based Method for Cloud Base Height Detection using Ceilometers: Application to Long-term observations in deriving Cloud Vertical Structure

Harshbardhan Kumar[1], V. Ravi Kiran[1], M. Venkat Ratnam[2], Herman Russchenberg[3], Arnoud Apituley[4]

[1]National Atmospheric Research Laboratory, Department of Space, Gadanki , 517 112, India.
[2]TU Delflt, Department of Geoscience and Remote Sensing, Delft, The Netherlands.
[3]Royal Netherlands Meteorological Institute (KNMI), Ministry of Infrastructure and Water management, Utrech, The Netherlands

Correspondence to: V. Ravi Kiran (ravikiranv@narl.gov.in)

Supplementary material

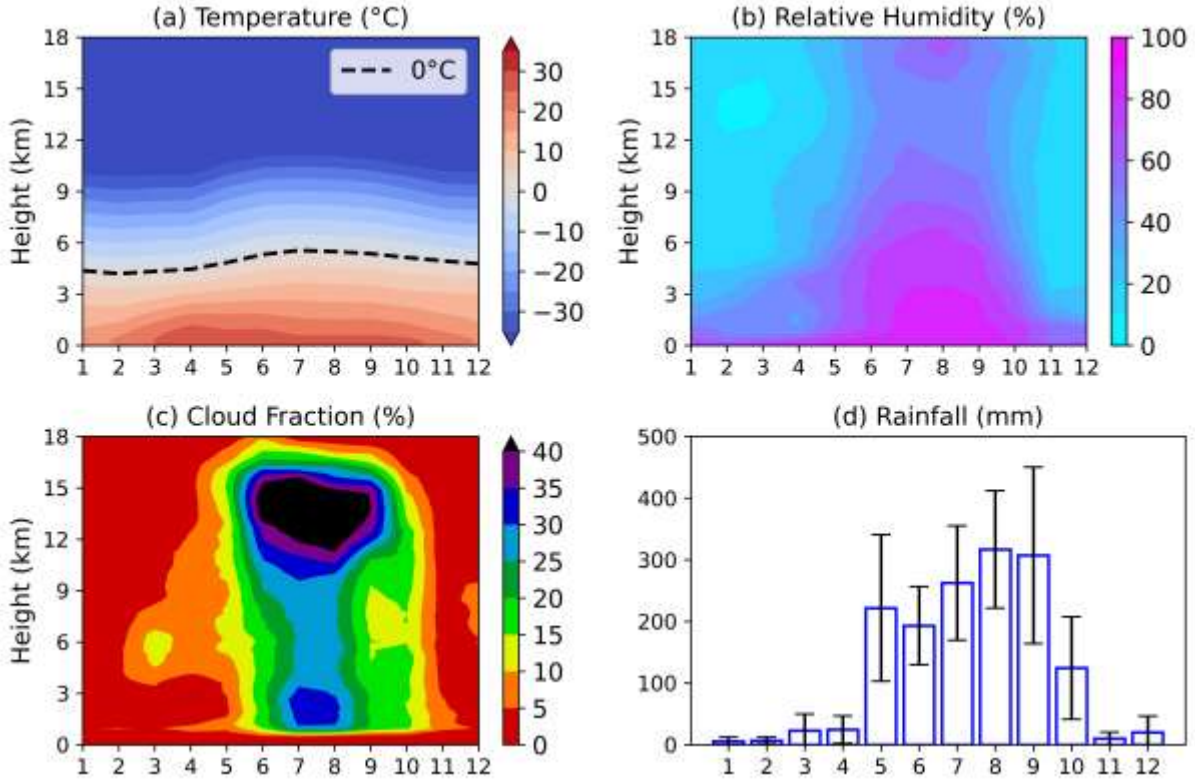

Figure S1. Monthly mean vertical profiles of (a) temperature, (b) relative humidity from radiosonde observations collected during January 2020 to December 2025 at 00UTC (05:30 IST), (c) cloud fraction as a function of altitude from combined CloudSat and CALIPSO observations for June 2006 to August 2020, and (d) rainfall records from KCON's automated weather station.

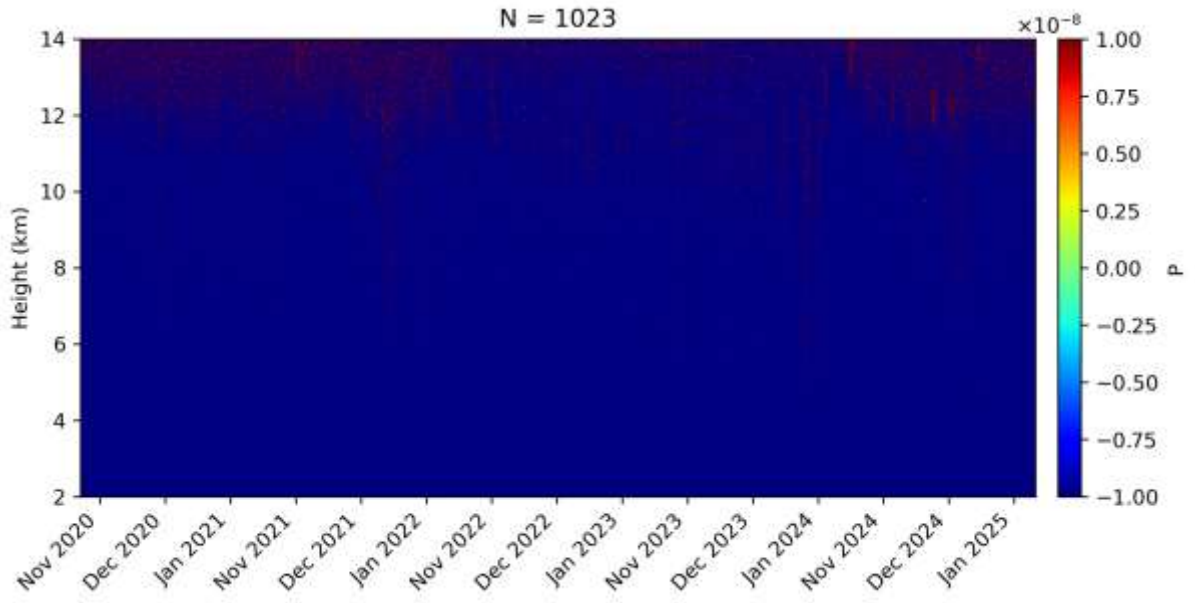

Figure S2. Time series of hourly mean of clear-sky mid-night (22:00 to 02:00 IST) non-range corrected signal (P) considered for dark current.

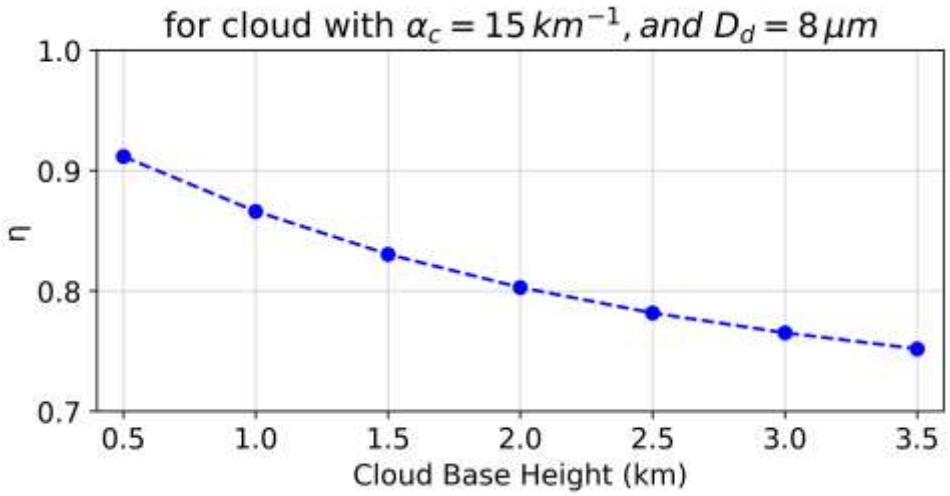

Figure S3. Multiple scattering correction factor (η) as function of cloud base height (taken from Marcos et al., 2018).

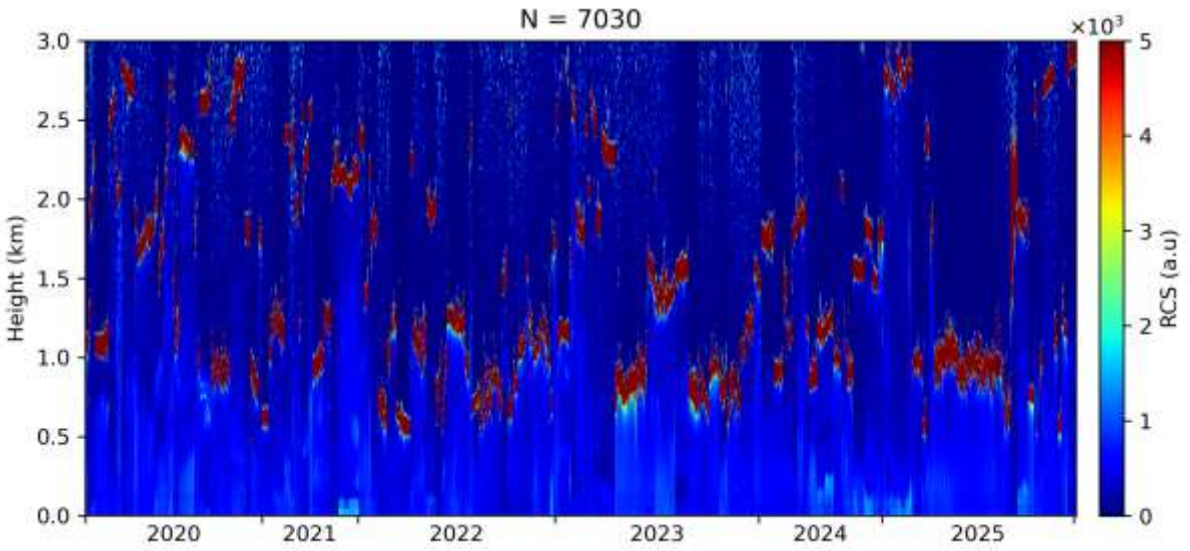

Figure S4. Time series of cloud profiles considered for the estimation of calibration factor (C).

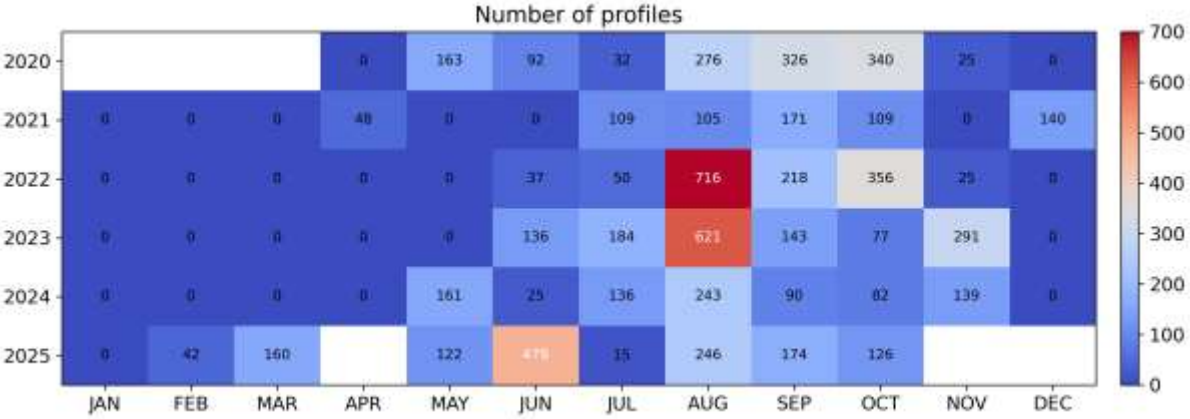

Figure S5. Year-month wise counts of cloudy profiles considered for the estimation of calibration factor.

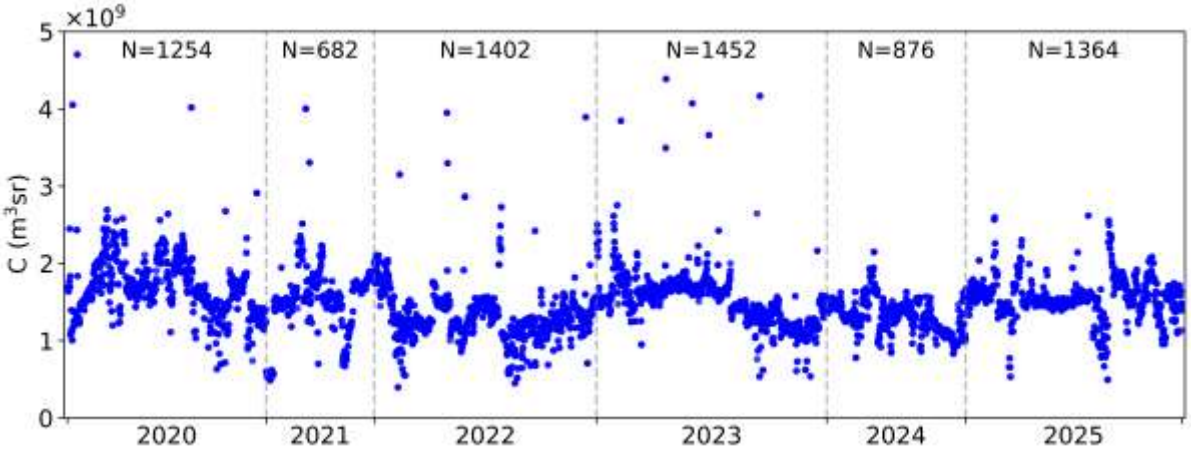

Figure S6. Temporal variation of estimated calibration factor for each cloudy profiles.

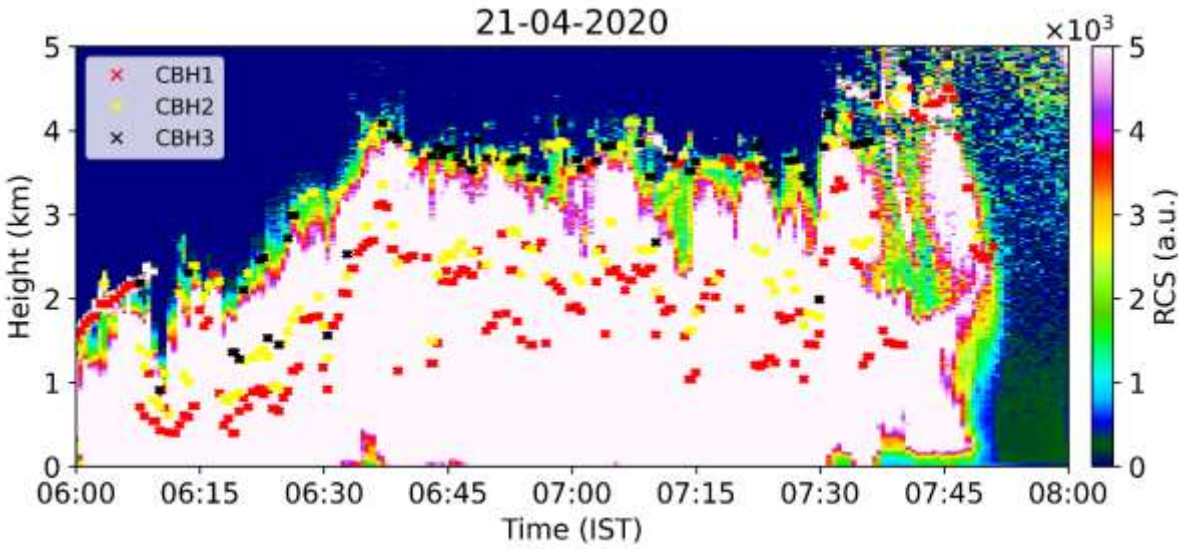

Figure S7. Example case showing CBH detection by CL51 algorithm in precipitation.

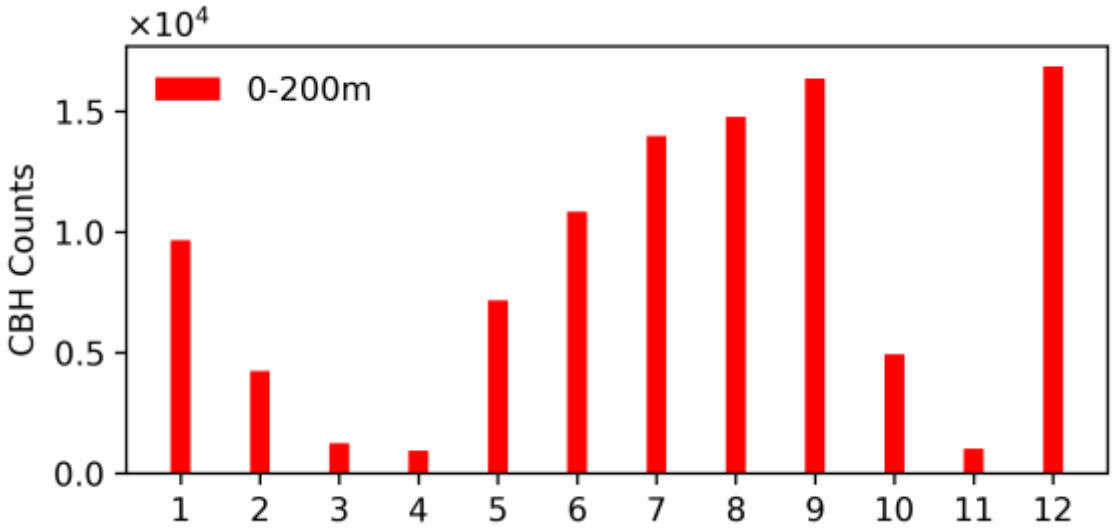

Figure S8. Month counts of CBH below 200m reported by CL51 algorithm during the study period.

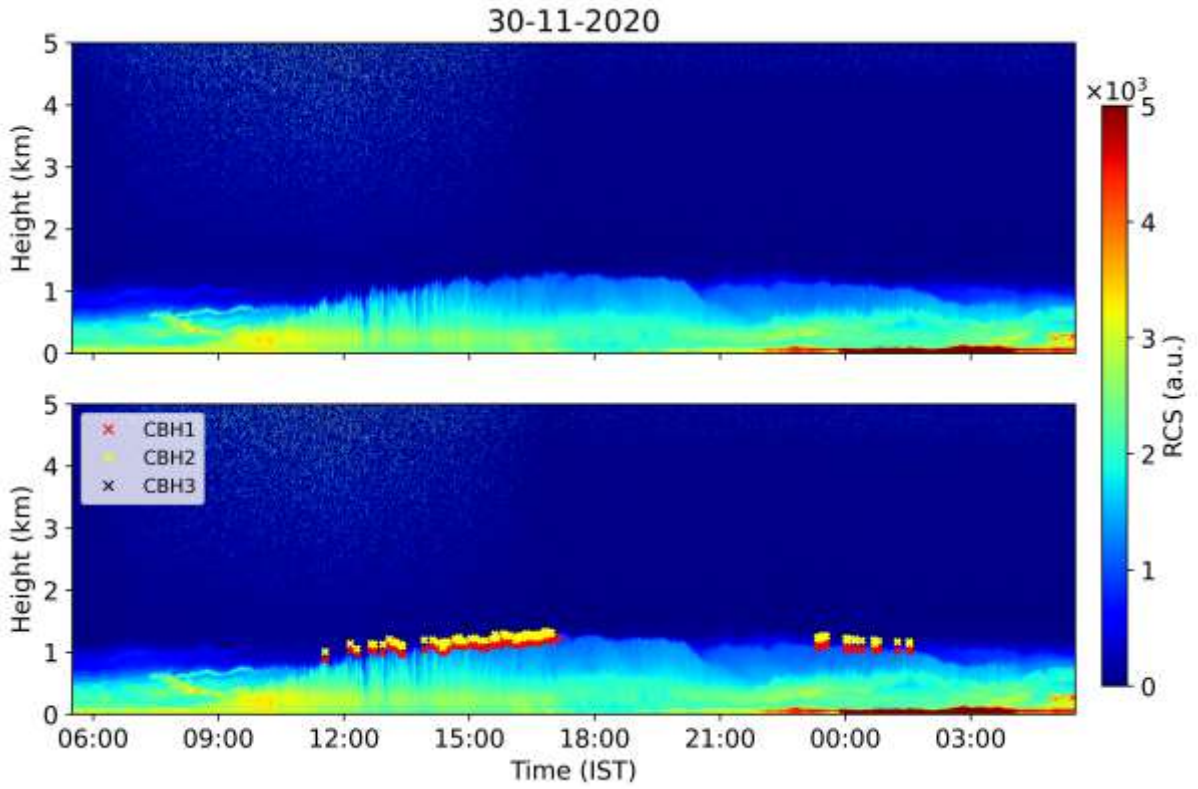

Figure S9. Range-corrected signal (RCS) from Vaisala CL51 observations on 30 November 2020 at KCON site, showing clear-sky boundary layer evolution through day and night (top panel). The bottom panel is same as top, showing RCS overlaid with CBH detected by the CL51 algorithm.

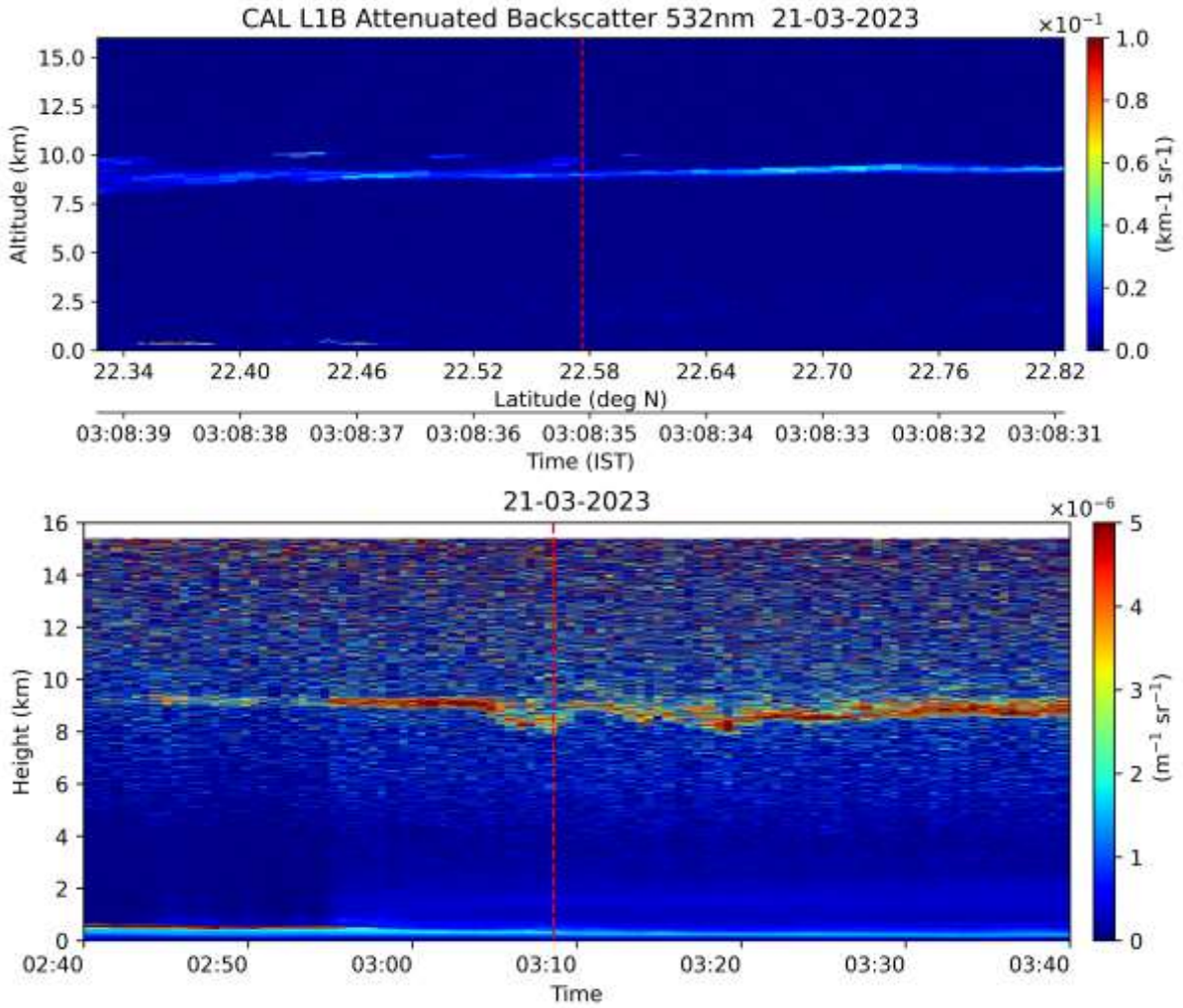

Figure S10. **Concurrent observations of cloud layers between 8 to 10 km on 21 March 2023 from a nearby night-time overpass of CALIOP/CALIPSO (top panel) and the CL51 ceilometer (bottom panel) at KCON measurement site. The red dashed line in the top panel indicates the CALIPSO track closest to the KCON site, while in the bottom panel it indicates the time of CALIPSO overpass.**

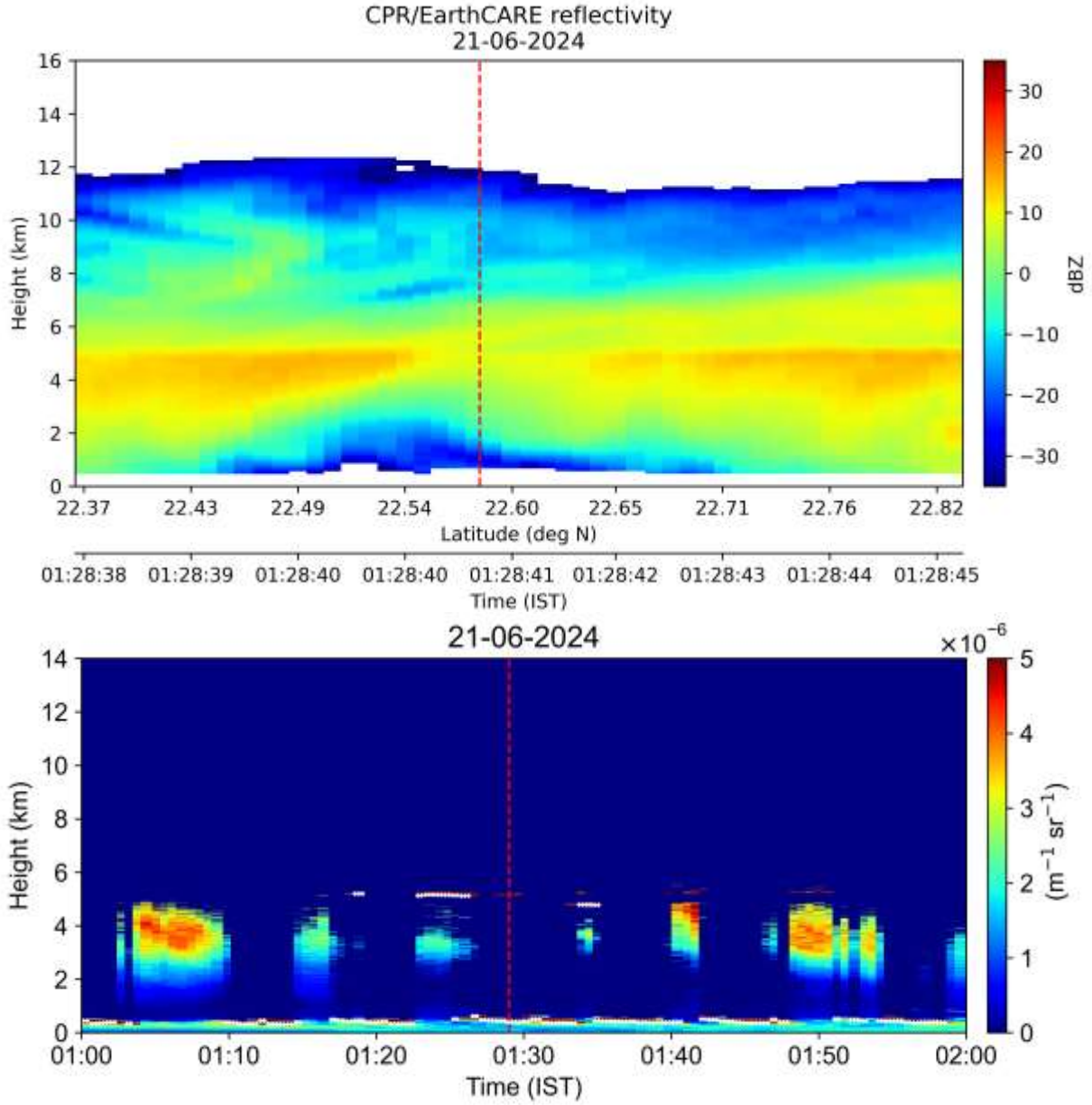

Figure S11. Concurrent observations of precipitating cloud layers on 21 June 2024 from a nearby night-time overpass of CPR/EarthCARE (top panel) and the CL51 ceilometer (bottom panel) at KCON measurement site. The red dashed line in the top panel indicates the EarthCARE track closest to the KCON site, while in the bottom panel it indicates the time of EarthCARE overpass.

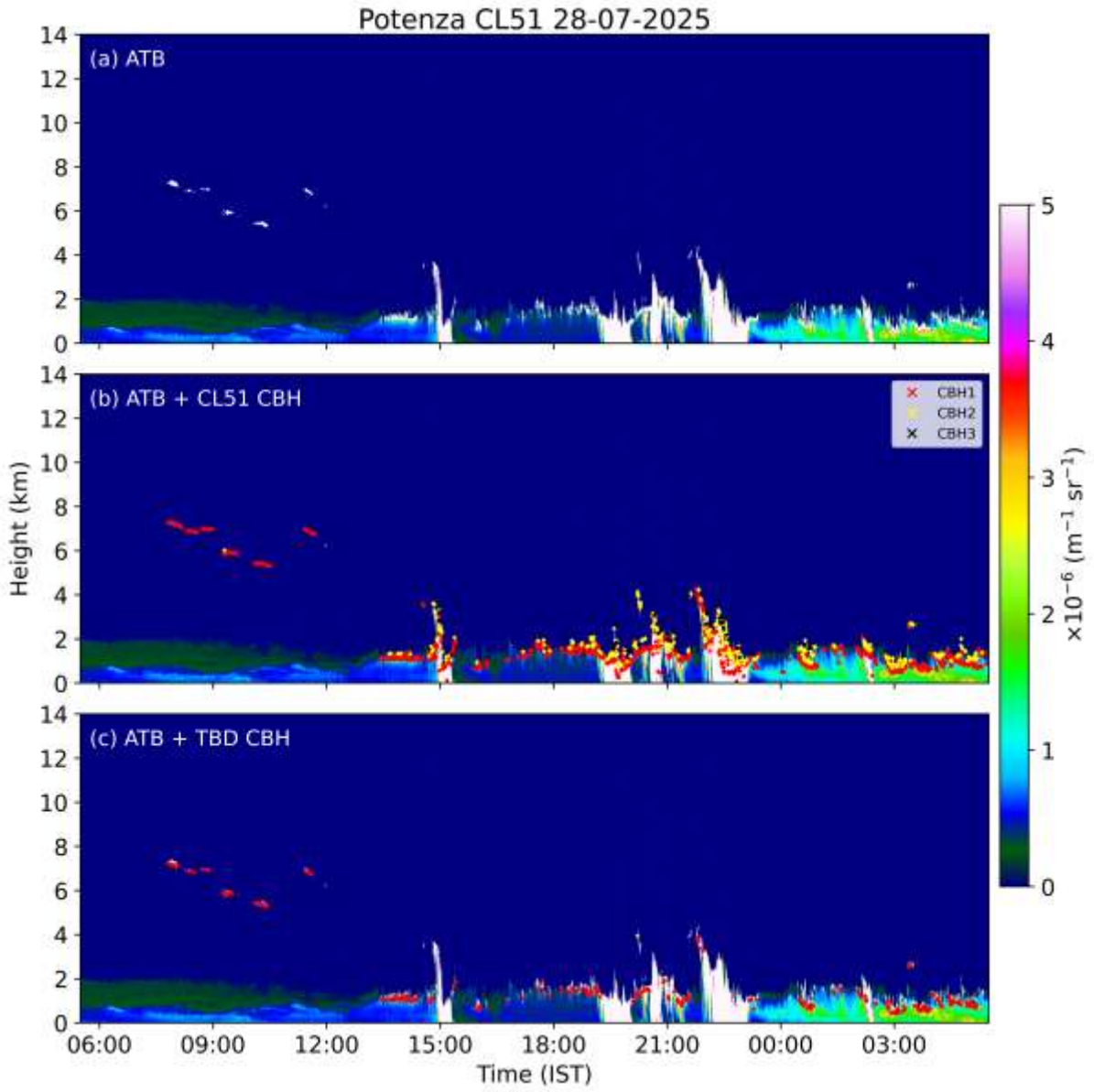

Figure S12. (a) Attenuated backscatter profiles from Vaisala CL51 observations on 28 July 2025 at the ACTRIS site in Potenza, Italy, overlaid with CBH detections shown as scatter points from (b) manufacturer's algorithm and, (c) TBD method.

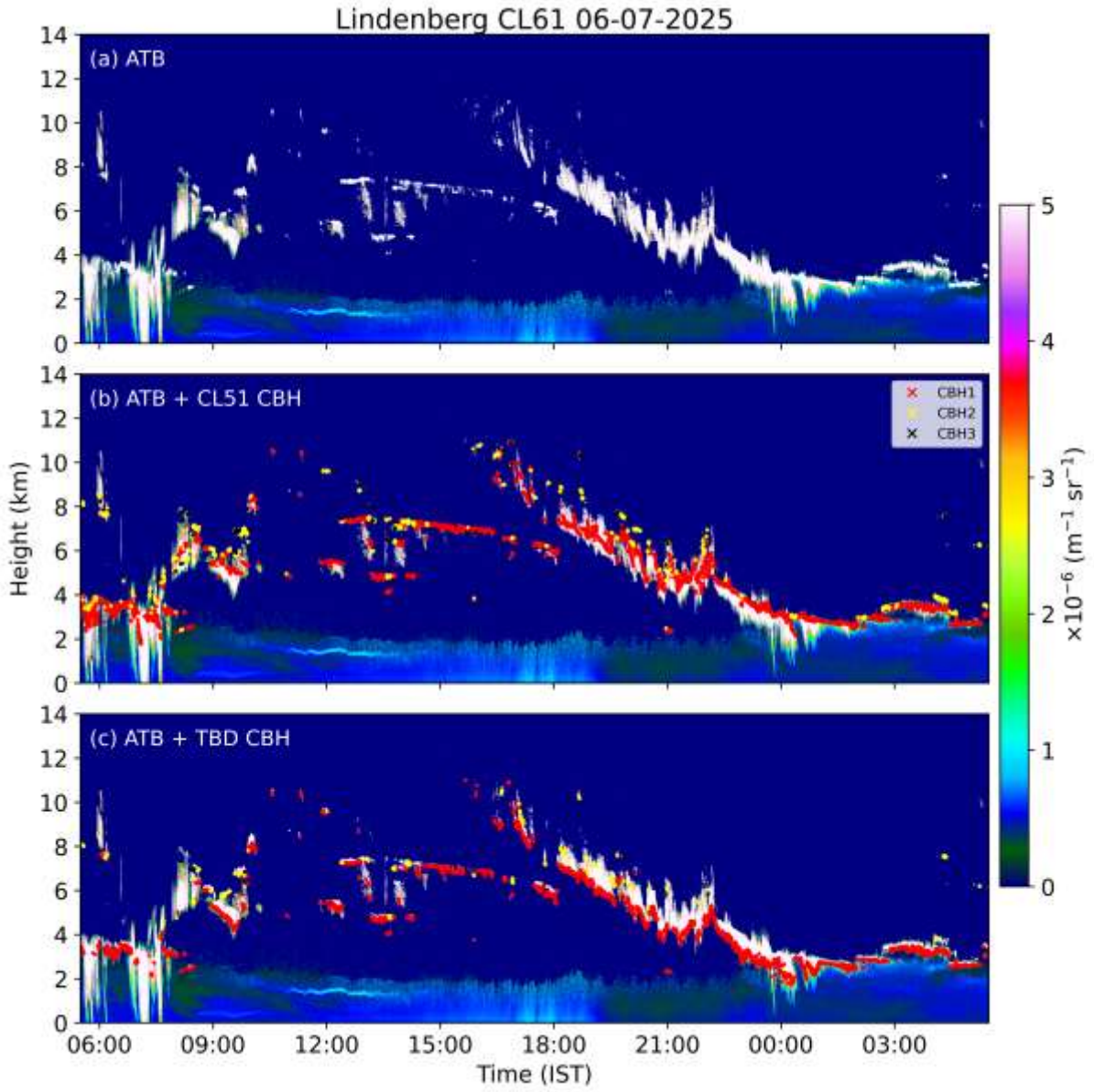

Figure S13. (a) Attenuated backscatter profiles from Vaisala CL61 observations on 7 June 2025 at the ACTRIS site in Lindenberg, Germany, overlaid with CBH detections shown as scatter points from (b) manufacturer's algorithm and, (c) TBD method.

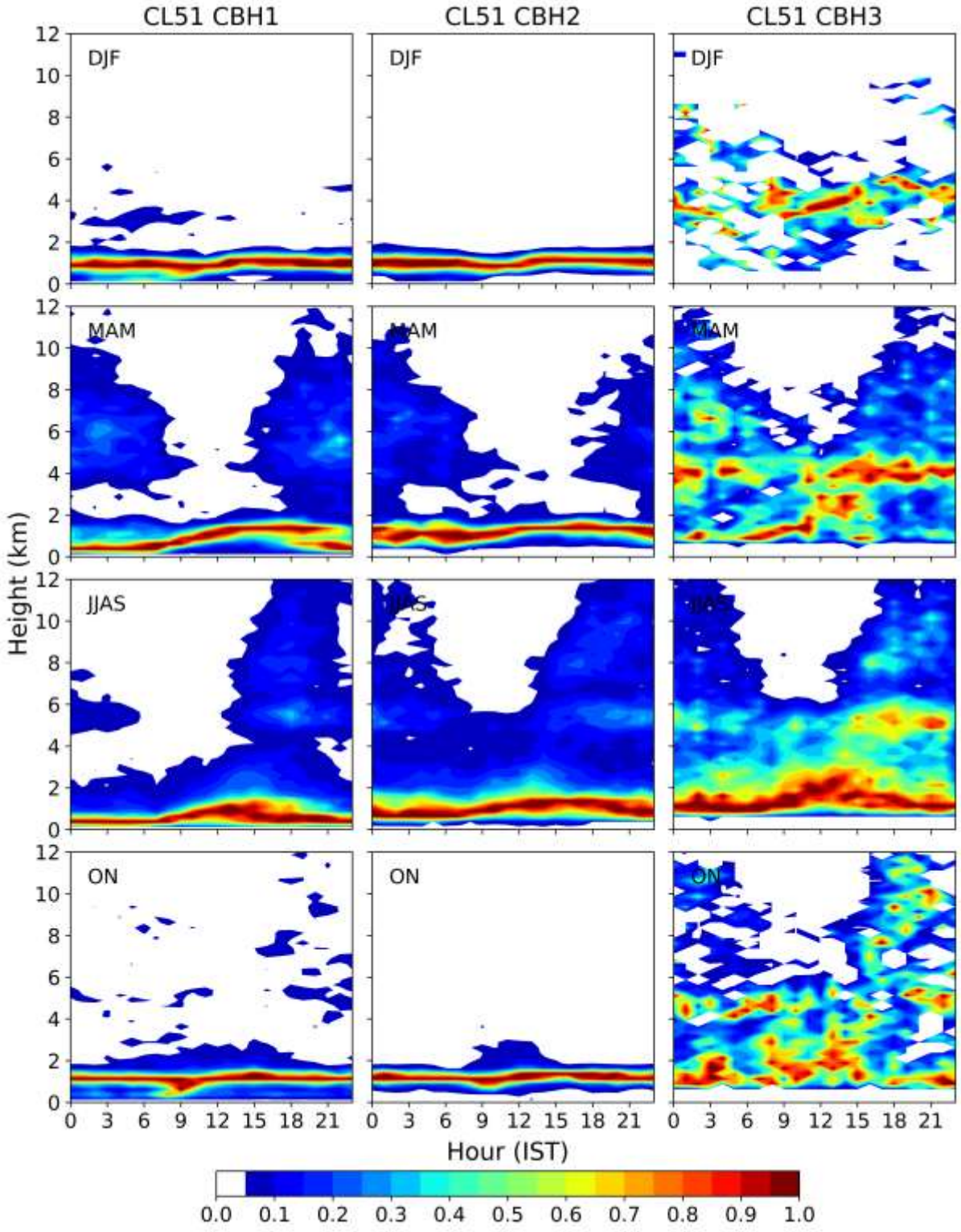

Figure S14. Season-wise hourly normalised occurrence of CBH reported by CL51 algorithm.